Temperature Dependence of Ion and Water Transport in Perfluorinated Ionomer Membranes for Fuel Cells

Morihiro Saito, Kikuko Hayamizu, and Tatsuhiro Okada*

National Institute of Advanced Industrial Science and Technology, AIST Tsukuba Center 5, Ibaraki 305-8565, Japan

Received: September 26, 2004; In Final Form: December 9, 2004

To clarify the mechanisms of transport of ions and water molecules in perfluorosulfonated ionomer membranes for fuel cells, the temperature dependence of their transport behaviors was investigated in detail. Two types of Flemion membranes having different equivalent weight values (EW) were utilized along with Nafion 117 as the perfluorinated ionomer membranes, and H-, Li-, and Na-form samples were prepared for each membrane by immersion in 0.03 M HCl, LiCl, and NaCl aqueous solutions, respectively. The ionic conductivity, water self-diffusion coefficient (D_{H2O}), and DSC were measured in the fully hydrated state as a function of temperature. The ionic conductivity of the membranes was reflected by the cation transport through the intermediary of water. Clearly, H^+ transports by the Grotthuss (hopping) mechanism, and Li^+ and Na^+ transport by the vehicle mechanism. The differences of the ion transport mechanisms were observed in the activation energies through the Arrhenius plots. The D_{H2O} in the membranes exhibited a tendency similar to the ionic conductivity for the cation species and the EW value. However, no remarkable difference of D_{H2O} between H- and the other cation-form membranes was observed as compared with the ionic conductivity. It indicates that water in each membrane diffuses almost in a similar way; however, H^+ transports by the Grotthuss mechanism so that conductivity of H^+ is much higher than that of the other cations. Moreover, the D_{H2O} and DSC curves showed that a part of water in the membranes freezes around −20 °C, but the nonfreezing water remains and diffuses below that temperature. This fact suggests that completely free water (bulk water) does not exist in the membranes, and water weakly interacting with the cation species and the sulfonic acid groups in secondary and higher hydration shells freezes around −20 °C, while strongly binding water in primary hydration shells does not freeze. The ratio of freezing and nonfreezing water was estimated from the DSC curves. The D_{H2O} in the membranes was found to be influenced by the ratio of freezing and nonfreezing water. DFT calculation of the interaction (solvation) energy between the cation species and water molecules suggested that the water content and the ratio of freezing and nonfreezing water depend strongly on the cation species penetrated into the membrane.

1. Introduction

Perfluorosulfonic acid polymer electrolyte membranes have attracted much attention in the past decade because of their wide applications in chlor-alkali electrolytes, water electrolysis, polymer electrolyte fuel cells (PEFC), and so on.[1−3] Especially, recent energy and environmental issues focus more on their roles in PEFC applications. However, they are still expensive for practical usage, and new advanced membranes with lower cost and higher performances, especially higher H^+ conductivity, are strongly desired. Actually, many studies have been done to date to realize such new advanced polymer membranes,[4,5] but only a very few candidates having higher performances than Nafion have been reported. To design advanced polymer membranes with new concepts, clarification of the mass transport mechanisms in the membranes having high performances, such as Nafion, is very valuable.

In the PEFC, H^+ conductivity and water diffusion in the membranes are closely related to each other, and the investigations of the behaviors of H^+ and water transports in the membrane are very important (Figure 1). As for their transport mechanisms in the Nafion, many studies have been done not only for single cation systems, especially the H-form membrane,[3,6−13] but also for binary cation systems.[14−20] We have also reported[21−26] the systematic investigations on various membrane properties, such as water content, ionic conductivity, water transference coefficient, and water permeability in H^+/alkali, H^+/alkaline earth, and H^+/transition-metal cation systems, especially to clarify the influences of the contaminant ions on the membrane properties.

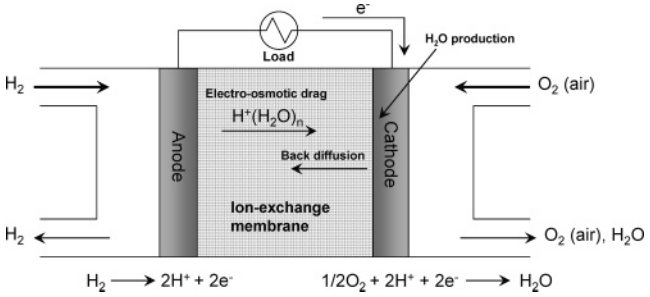

Figure 1. Schematic illustration of H^+ and water transport within a PEFC.

However, these studies mainly utilized Nafion 117, and its equivalent weight value (EW), which is equal to the inverse of

* Corresponding author. Telephone: + 81 29 861 4464. Fax: +81 29 861 4678. E-mail: okada.t@aist.go.jp.

10.1021/jp045624w CCC: $30.25
Published on Web 02/01/2005

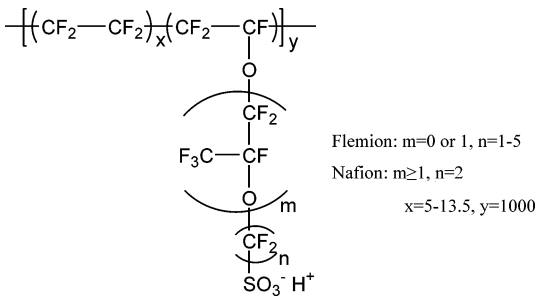

Figure 2. Structures of polymer membrane of Flemion and Nafion in the H-form state.

the ion-exchange capacity (IEC) of the membrane, is basically constant as 1100 g equiv^{-1}. Therefore, the investigation of membranes having different EW values is quite important for further understanding of the relationships between the structure of the membranes and the transport behaviors of carrier cations and water. Recently, we utilized various types of perfluorosulfonic acid polymer membranes such as Aciplex and Flemion having different EW values along with Nafion 117 and reported on their transport behaviors in the H-, Li-, and Na-form membranes at room temperature.[27]

In the present study, as a succeeding investigation, we examine the temperature dependence of their transport behaviors to understand thermal properties of the polymers. The ionic conductivity and the water self-diffusion coefficient in the membranes were evaluated and discussed for ions and water transport mechanisms. The state of water in the membranes was also investigated by DSC measurement. The freezing and nonfreezing water in the membranes at low temperature as well as the interaction energy between the cation species and water molecules were estimated by DSC and DFT calculations, respectively. From these data, the relationships between the membrane structure, the water condition, and their transport behaviors are discussed.

2. Experimental Section

2.1. Membrane Preparation. Flemion SH-120 (EW 909) and LSH-180 (EW 1099), from Asahi Glass Co., Ltd. (Yokohama, Japan), and Nafion 117 (EW 1100), from DuPont (Wilmington, DE), were utilized as perfluorosulfonated ionomer membrane samples. Hereafter, the Flemion SH-120 and LSH-180 membranes are represented as Flemion 120 and Flemion 180, respectively. The structures of the membranes are shown in Figure 2. The membranes were pretreated according to the reported procedure.[27] After the pretreatments, the membranes were immersed in 0.03 M HCl, LiCl, and NaCl aqueous solutions for one month to exchange the countercation in the membranes; the aqueous solutions were changed to new ones every week.[27]

2.2. Ionic Conductivity Measurements. The impedance of the membranes was measured in the lateral direction using a Solartron S-1260 frequency response analyzer (Solartron Instrument) with 20 mV ac modulation over a frequency range from 10^6 to 10^{-1} Hz with the open-circuit potential. The measurement was made by using a homemade Teflon cell described in our previous paper.[22] The electrode was black-platinized Pt foil contacting the membrane on each of two sides with 10 mm width and 5 mm separation. During the measurement, the membranes were in a hydrated state in contact with equilibrating ionic solution by way of a 10 × 5 mm window on each side. The measurement was carried out in the temperature range 50−10 °C, after the sample in the cell was heated to 50 °C. The specific conductivity of the membranes κ (S cm^{-1}) was obtained from the real part of the impedance R (Ω) of the membranes:

$$\kappa = \frac{0.5}{Rl} \tag{1}$$

where l is the thickness (cm) of the membranes, which was measured for each sample by a micrometer.

2.3. Self-Diffusion Coefficient Measurements. The self-diffusion coefficients of the water (^{1}H) and the Li$^+$ (^{7}Li) in the membranes were measured by the pulsed-gradient spin−echo (PGSE)-NMR method[27] using a JEOL GSH-200 spectrometer with a 4.7 T wide bore superconducting magnet equipped with a Techmag Apollo and a NTNMR. The measurements were performed in the temperature range 30 to −40 °C. The pulse sequences for the measurements were a modified Hahn spin−echo sequence (i.e., 90°-τ-180°-τ-acq) for the diffusion of water and a stimulated echo-based sequence for the diffusion of Li$^+$, respectively. The free diffusion echo signal attenuation E obtained by using those pulse sequences obeys the following equation:

$$\ln(E) = \ln(S/S_{g=0}) = -\gamma^2\delta^2 g^2 \mathrm{D}(\Delta - \delta/3) \tag{2}$$

where S is the spin−echo signal intensity, γ is the gyromagnetic ratio (rad s^{-1} T^{-1}), δ (s) is the duration of the field gradient pulse with magnitude g (T m^{-1}), D is the self-diffusion coefficient of the species, and Δ (s) is the duration between the leading edges of the two gradient pulses. The measurements were conducted by setting g = 0.99 to 3.05 T m^{-1} for ^{1}H and 7.19 T m^{-1} for ^{7}Li, respectively. The E was measured as a function of δ to estimate the diffusion coefficients of water (D_{H2O}) and of Li$^+$ ($D_{\mathrm{Li+}}$) in the membranes by using eq 2. The self-diffusion coefficient of Na$^+$ in the membranes could not be measured because of the large line width of the ^{23}Na NMR spectrum. The samples for NMR measurements were prepared by using a 5-mm tube and put the membrane with a 5-mm height after wiping to remove H_2O outside of the membrane.

2.4. DSC Measurements. The thermal properties of water in the membranes were investigated by differential scanning calorimetry (DSC) using a DSC 6220 (Seiko Instruments). The measurements were carried out from 50 to −50 °C at the scan rate of 1 °C min^{-1}, after the sealed sample in the aluminum pan was heated to 50 °C at the same scan rate. An empty aluminum pan was used as a reference.

2.5. Interaction Energy Calculations. Gaussian 03 program[28] was used for the DFT calculations. The geometry of the cation/water clusters [$X^+/(H_2O)_n$; $X^+ = H_3O^+$, Li$^+$, and Na$^+$; n = 1−4] were optimized at the B3LYP/6-311+G** level. The intermolecular interaction energies among the cation and water molecules were calculated at the same level. The basis set superposition error (BSSE)[29] was corrected for all calculations using the counterpoise method.[30]

3. Results

3.1. Ionic Conductivity. Figure 3 shows the Arrhenius plots of ionic conductivity κ for the prepared membrane samples in the temperature range 50−10 °C. The values of κ in the H-form membranes were four to five times larger than those of the Li- and Na-form ones. It indicates that the H$^+$ in the membranes might transport by the Grotthuss (hopping) mechanism,[31] and Li$^+$ and Na$^+$ by the vehicle mechanism.[32] In addition, the ionic conductivity increased with decreasing EW value regardless of the cation species. In our previous study,[27] various types of perfluorinated ionomer membranes such as a Nafion, two

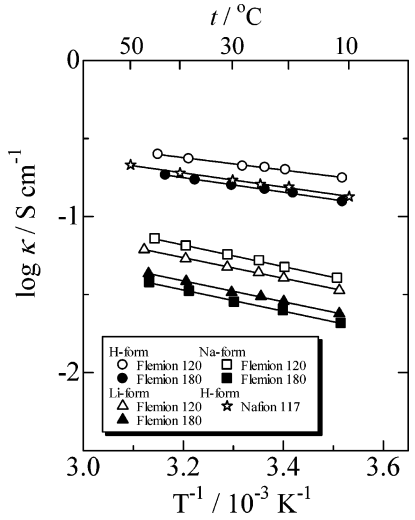

Figure 3. Arrhenius plots for ionic conductivities κ of Flemion X-form membranes having different EW values along with Nafion 117 H-form membrane in the fully hydrated state with the corresponding ionic solution.

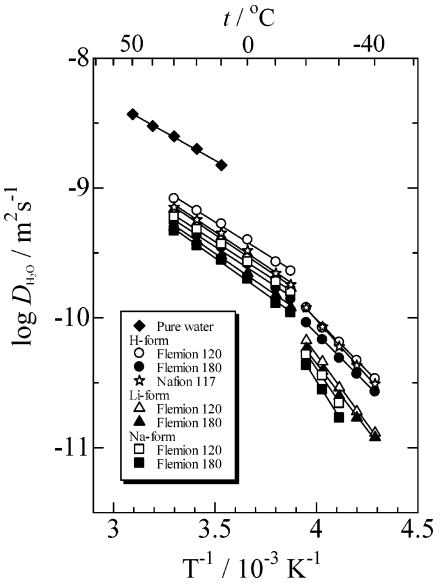

Figure 4. Arrhenius plots for water diffusion coefficients D_{H_2O} of Flemion X-form membranes having different EW values along with Nafion 117 H-form membrane.

Aciplex, and four Flemion having different EW values, including Flemion 120 and 180, showed the same tendency between the EW value and the ionic conductivity at 25 °C. The same dependences of the ionic conductivity on the cation species and the EW value were confirmed for the whole measuring temperature range of 50−10 °C. The increase in the ionic conductivity with decreasing EW value arises from the increase in the water content in the membranes,[27] which is due to the increase in the number of cations and sulfonic acid groups having high hydrophilic properties. Measured values of the ionic conductivity for the Nafion 117 H-form membranes in the present study were higher than those reported in the previous papers.[33,34] This difference would be due to the difference in experimental conditions where membranes were all in contact with the equilibrating solutions on both sides. With this regard, we compare the values of the ionic conductivity obtained at the same experimental conditions.

3.2. Water Self-Diffusion Coefficient. Figure 4 shows the Arrhenius plots of the D_{H2O} for the membranes in the temperature range 30 to −40 °C along with that for pure water. All of the plots follow similar trends from 30 to −15 °C and the values were about three to five times lower than that for pure water. Around −20 °C, the signal intensity decreased and the line width increased. The D_{H2O} also discontinuously decreased and followed steeper temperature dependence than those above −15 °C. These facts mean that the water in the membranes above −15 °C moves like bulk water but the mobility is limited. The water in the membranes is partially frozen around −20 °C, but nonfrozen water remains in the all membranes and moves in the membranes below that temperature. The D_{H2O} increased with decreasing EW values, and the H-form membranes exhibited higher values than those of the Li- and Na-form ones in the whole temperature range. These results are in good agreement with those of the ionic conductivity in the temperature range between 30 and 10 °C and are consistent with the results of the previous study at 30 °C.[27] However, different from the ionic conductivity, no remarkable difference of D_{H2O} was observed between H- and the other cation-form membranes. It indicates that water in the membranes diffuses almost in the similar way, but the H^+ transports by the Grotthuss mechanism so that the H^+ conductivity is much higher than that of the other cations. Cappadonia et al.[9] studied the temperature dependence of H^+ conductivity for Nafion 117 membrane from 27 to −133 °C, where the membranes were pretreated with various conditions. They showed that the values follow the different Arrhenius plots above and below around −13 °C, including the discontinuous decrease around −13 °C for all the membranes. These tendencies are in good agreement with the present D_{H2O} behaviors. Therefore, the drastic decrease in the H^+ conductivity reported by Cappadonia et al. can be interpreted as arising from the decrease in the water diffusion rate due to the partial freezing of water in the membranes.

3.3. Li^+ Self-Diffusion Coefficient. The PGSE-NMR method can afford the self-diffusion coefficients of both water and ion individually in electrolyte systems and is quite effective in the investigation of transport mechanisms in the membranes because the water and ion diffusion can be compared directly. Here, to clarify the relationships between the mobility of water and the cation species in more detail, Li^+ self-diffusion coefficients D_{Li+} in the Li-form membranes were measured and compared with D_{H2O}.

Figure 5 shows the Arrhenius plots of D_{Li+} for the Flemion Li-form membrane along with those of D_{H2O}. As shown in Figure 5, the plots follow two straight lines with discontinuities around −20 °C and D_{Li+}-value increases with decreasing EW value as well as D_{H2O}, although the D_{Li+} values were about four times smaller than the D_{H2O} above −15 °C. The Li^+ transport is influenced by the solvating water molecules (at least in a certain time/length scale), which results phenomenologically in a lower Li^+ diffusion coefficient compared to the diffusion coefficient of the water molecules. The D_{H2O} measured by the PGSE-NMR is the weighted average value of the D values of bulk water and the solvating water with the ions. Therefore, the D_{Li+} was smaller than the D_{H2O}, although the temperature dependences were similar to each other. Below −20 °C, D_{Li+} could not be obtained because the T_2 of the ^{7}Li NMR drastically became short (increase in line width) and D_{Li+} would also drastically decrease below −20 °C, similar to D_{H2O}.

3.4. DSC Curve of the Membranes. The states of water in the membranes were examined by DSC measurement. Figure 6 shows the DSC curves for nine membranes under study. For all of the membranes, no peak was observed between 50 and −15 °C, and around −20 °C a peak due to the freezing of water

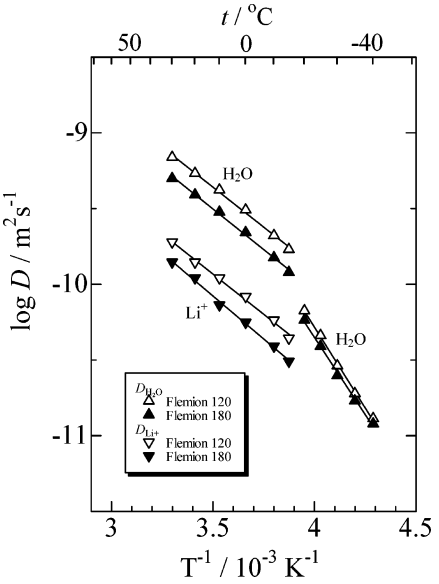

Figure 5. Arrhenius plots for diffusion coefficients of water D_{H_2O} and Li^+ D_{Li^+} in Flemion Li-form membranes having different EW values.

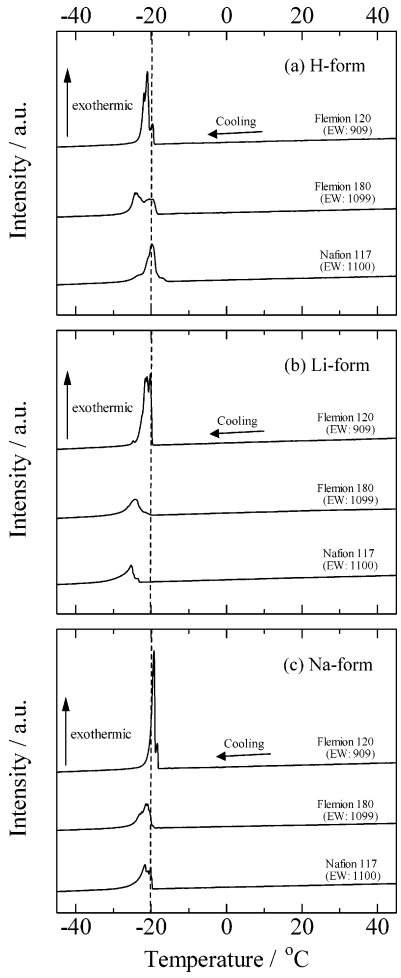

Figure 6. DSC curves of Flemion X-form membranes having different EW values along with Nafion 117 X-form membrane in the fully hydrated state measured in the temperature-decreasing process.

appeared. This is in good agreement with the result of the water self-diffusion coefficient in the membranes. As mentioned above in section 3.2, a part of water in the membranes freezes around −20 °C. The DSC peaks correspond only to the freezing water, which is weakly interacting water with the cation species and

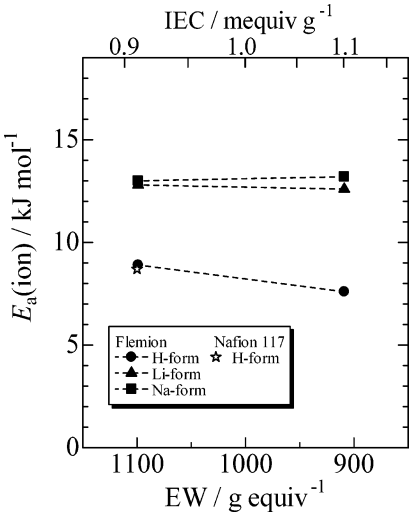

Figure 7. Activation energies for ion transports E_a(ion) within Flemion X-form membranes against the EW value of the membranes along with Nafion 117 H-form membrane in the fully hydrated state.

the sulfonic acid groups in secondary and higher hydration shells. Some peaks due to the freezing water split and scattered relatively widely. This indicates the existence of several kinds of water molecules in different states. Generally, water in an aqueous ionic solution is supercooled by the strong interaction with ionic species. In perfluorosulfonated membranes, water forms ionic clusters like a Gierke model[35] and countercations dissociated from sulfonic acid groups exist relatively near the sulfonic acid groups. The water influenced by these ionic species would not easily freeze, while water far from the ionic species would be relatively easier to freeze. The height and the area of the peaks were larger for the membranes having a lower EW value, regardless of the cation species. This fact suggests that the amount of water weakly interacting with the ionic groups increases with decreasing EW value. This is in good agreement with the result of the D_{H2O} in section 3.2, where the D_{H2O} increased with decreasing EW value.

4. Discussion

4.1. Activation Energy for Ion Transport. The activation energies for ion transports E_a(ion) are plotted in Figure 7 against the EW value. The values were calculated from the Arrhenius plots of ionic conductivity in Figure 3. The activation energy for the H-form membranes was much smaller than those for the Li- and Na-form ones and decreases with decreasing EW value, while those for Li- and Na-form ones were almost constant. The results imply that H^+ moves by two transport mechanisms, i.e., Grotthuss and vehicle mechanisms, as shown in Figure 8. The ratio of the transportation by the Grotthuss mechanism would increase with decreasing EW value because the water content in the membranes increases with decreasing EW value,[27] while Li^+ and Na^+ move dominantly by the vehicle mechanism. Our results for H-form membranes are consistent with Zawodzinski et al.'s studies[7] on the Nafion 117 H-form membranes having different water content at 30 °C. They also reported that H^+ in the Nafion moves by both Grotthuss and vehicle mechanisms and the ratio of the transportation by the Grotthuss mechanism increases with an increase of the water content in the membrane.

4.2. Activation Energy for Water Transport. The activation energies for water transport in the membranes $E_a(H_2O)$, which were calculated from the Arrhenius plots of water self-diffusion coefficients in Figure 4, were shown in Figure 9(a) and (b).

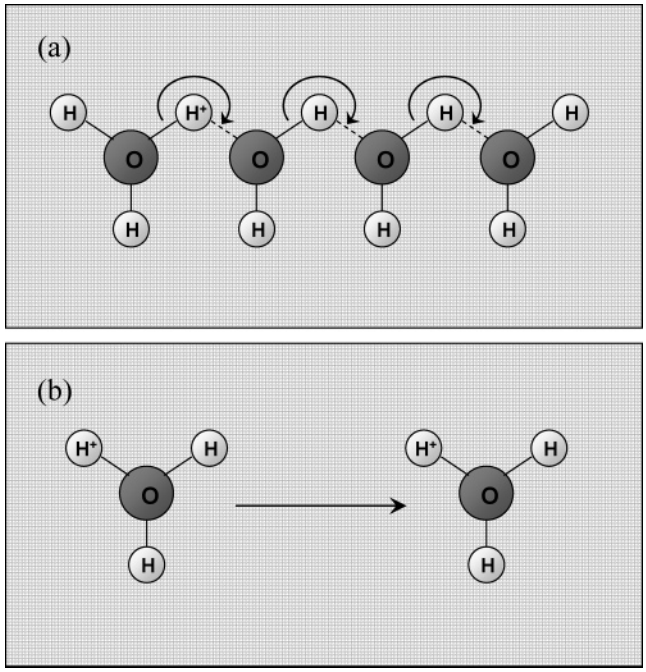

Figure 8. Models of H^+ transport mechanisms within perfluorosulfonated ionomer membranes in the fully hydrated state. (a) Grotthuss (hopping) and (b) vehicle mechanisms. (a) is a simplified model of the Grotthuss mechanism, where the proton hopping direction deals with only one dimension.

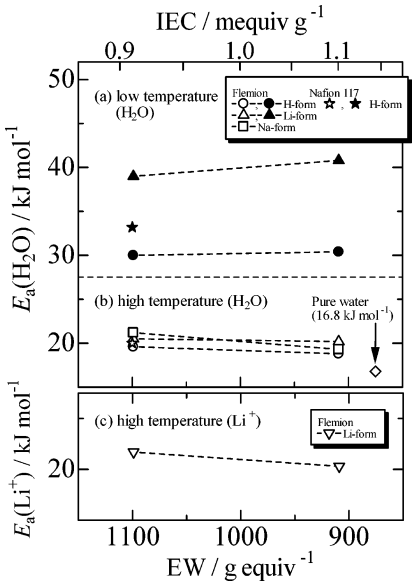

Figure 9. Activation energies for the transports of water $E_a(H_2O)$ and Li^+ $E_a(Li^+)$ in Flemion X-form membranes plotted against the EW value of the membranes along with Nafion 117 H-form membrane.

The different values were obtained for the temperature ranges between 30 and −15 °C and below −20 °C. At the high-temperature range, the $E_a(H_2O)$ values were smaller than those obtained for the low-temperature range and decreased with decreasing EW value to approach the value for pure water. The H-form membranes gave slightly smaller values than the other cation-form membranes. The water in the membrane having lower EW value moves easily, especially in the H-form one. On the other hand, at the low-temperature range, the $E_a(H_2O)$ values became much larger and increased with decreasing EW value for H- and Li-form membranes. In addition, the difference between the H- and Li- membranes became larger than those at the high-temperature range. As mentioned above in section 3.2, the water in the membranes is partially frozen around −20 °C, and nonfreezing water remains and moves below this temperature. Therefore, in the low-temperature range, the E_a-(H_2O) represents the activation energy for the transportation of the nonfreezing water, which is water that is strongly binding to the cation species or the sulfonic acid groups in primary hydration shells. The results of Figure 9(a) imply that it is more difficult for the nonfreezing water to move in the membranes having lower EW value (indicating the larger amount of ionic groups), although the net D_{H2O} is slightly higher. In addition, the nonfreezing water in the Li-form membranes is binding stronger to the ionic groups than those in the H-form membranes.

4.3. Activation Energy for Li^+ Transport by the PGSE-NMR Method. Figure 9(c) shows the activation energy for Li^+ transport $E_a(Li^+)$ in the Flemion Li-form membranes estimated from Li^+ diffusion coefficients in Figure 5 in the higher-temperature range. As shown in Figure 9(c), the values were slightly larger than $E_a(H_2O)$ and decreased with decreasing EW value as well as the $E_a(H_2O)$. These facts also support the concept that Li^+ transports by vehicle mechanism in the membranes.

4.4. Diffusion Radius of Li^+. The rate of the ion transport is related to the water diffusion rate, which is influenced by the interaction of water with the cation species and the sulfonic acid groups. Especially, the states of water molecules in the membranes depend on the cation species. We utilize the Li-form membranes as a representative system and estimate the Li^+ diffusion radius. The water coordination number for Li^+ was obtained by using the D_{H2O} and D_{Li+} values from the PGSE-NMR measurements.

The translational diffusion of a species can be expressed by the Stokes−Einstein equation,[36,37]

$$D = \frac{kT}{\alpha \pi \eta r_s} \tag{3}$$

where k is Boltzmann's constant (1.3807×10^{-23} J K^{-1}), T is the temperature (K), η is the solution viscosity (Pa s^{-1}), and r_S is the Stokes (or effective hydrodynamic) radius (m). α is a constant which ranges from 4 (slipping) to 6 (stick) for perfect slipping conditions.[38] We note that the Stokes−Einstein equation is not strictly applicable to the electrolyte systems, but at a semiquantitative level it provides valuable insight. Assuming α and η are the same for the H_2O and Li^+ diffusion, from eq 3 it can be seen that the ratio

$$R = D_{H2O}/D_{cation} = r_{cation}/r_{H2O} \tag{4}$$

is a measure of the radius of the diffusing cations relative to that of a water molecule. The R value is an average value for diffusing cation species because the PGSE-NMR method reflects an average value of self-diffusion coefficients of species.

Figure 10 shows the Li^+ diffusion radius R in Flemion Li-form membranes plotted against the temperature. The values were around four and almost constant against the temperature, regardless of the EW value. This means that about four water molecules coordinate around a Li^+ in both membranes, which agrees with the number of primary shell water molecules directly coordinating Li^+ in the gas phase[39] and aqueous solution.[40] Therefore, the Li^+ in the membranes is solvated by about four water molecules and moves by the vehicle mechanism.

4.5. Freezing and Nonfreezing Water in the Membranes. For further understanding of the states of water in the mem-

TABLE 1: Water Conditions in Flemion Membranes along with Nafion 117 in the Fully Hydrated State

membrane	Flemion 120 (EW: 909)			Flemion 180 (EW: 1099)			Nafion 117 (EW: 1100)		
X-form	H	Li	Na	H	Li	Na	H	Li	Na
freezing enthalpy (J g^{-1})[a]	37.0	47.1	44.7	29.9	22.0	26.6	30.2	19.4	29.4
water content λ[b,c]	23.6	25.9	21.1	19.1	20.3	17.0	20.8	24.3	20.1
freezing water[c]	8.3−8.9	10.8−11.6	9.8−10.5	7.2−7.7	5.4−5.8	6.3−6.8	7.7−8.3	5.0−5.4	7.3−7.8
nonfreezing water[c]	14.7−15.3	14.3−15.1	10.6−11.3	11.4−11.9	14.5−14.9	10.2−10.7	12.5−13.1	18.9−19.3	12.3−12.8
average ratio of freezing water	0.37	0.43	0.48	0.39	0.27	0.39	0.39	0.21	0.37

[a] Calculated from the area of DSC peaks for the water freezing. [b] Ref 27. [c] Number of water molecules per cation exchange site.

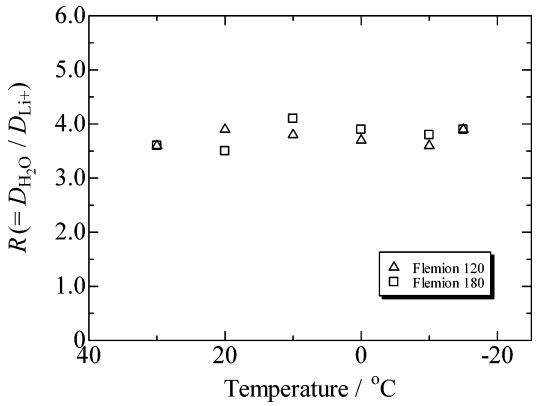

Figure 10. Li^+ diffusion radii R in Flemion Li-form membranes.

branes, the amount of freezing and nonfreezing water were estimated from the freezing peak area in the DSC curves by using the method of our previous paper.[22] Generally, the freezing water in the membranes must have certain crystalline structures which are assumed to be the same as the structures of natural ice. There are nine polymorphic forms of the natural ice: I, Ic, II, III, IV, V, VI, VII, and VIII.[41] The structures of ice-forms IV−VIII are formed only under very high pressures. Therefore, in the present experimental conditions, the possible structures of ice for the freezing water in the membranes are I, Ic, II, and/or III. The melting enthalpy ranges are between 334 (ice I) and 311 J g^{-1} (ice III). The number of freezing water N_{fre} (per cation exchange site) can be calculated from the area of the freezing peak of water in the DSC curves (Figure 6) using the melting enthalpy of ice I and III H_{ice} as follows:

$$N_{fre} = \frac{W_{fre}}{W_{tot}} \times \lambda = \frac{H_{fre}/H_{ice}}{(W_{wet} - W_{dry})/W_{wet}} \times \lambda \qquad (5)$$

Here, W_{fre} and W_{tot} are the weights of freezing and total water included in each membrane, respectively. λ is the total water content (per cation exchange site) in the membranes. H_{fre} (J g^{-1}) is the freezing enthalpy of water per gram of the membrane estimated from the area of freezing peak of water. W_{wet} and W_{dry} are the weight of the membranes in the fully hydrated and dry states, respectively. W_{wet}, W_{dry}, and λ were measured in our previous study.[27] Since the H_{ice} values are given in the range 334 to 311 J g^{-1}, the N_{fre} values are also calculated in the range. The number of nonfreezing water N_{non} (per cation exchange site) was taken as the difference between the total water content λ and the number of freezing water N_{fre}. The results are summarized in Table 1.

For all of the membranes, the number of freezing water molecules increased with decreasing EW value, independent of the cation species. This fact can explain the trend that D_{H2O} increases with decreasing EW value, because the freezing water corresponds to water weakly interacting with the ionic groups in the membranes as compared with nonfreezing water. Especially in the Li- and Na-form membranes, the number of nonfreezing water molecules was almost constant for each cation-form membrane, although the number of freezing water molecules increased with decreasing EW value. It implies that the number of nonfreezing water mainly depends on the cation species, while the number of freezing water depends on the EW value. On the other hand, in the H-form membranes, both numbers of freezing and nonfreezing water molecules increased with decreasing EW value, and the average ratio was almost constant. This indicates that H^+ in the membranes exists as H_3O^+ and the rate of proton exchange with H_2O is quite fast and undistinguishable. This also supports the concept that H^+ in the membranes transports mainly by the Grotthuss mechanism.

4.6. Interaction between Cation Species and Water Molecules. As mentioned in the above sections, water transport is closely related to ion transport inside the membranes. In addition, water transport in the membranes is strongly influenced by the interaction with the ionic species, i.e., cations and sulfonic acid groups. Especially the cation species and their hydrophilic property are quite important for the water content and mobility.[21−27] In section 4.4, for the Li-form membranes, the water coordination number of Li^+ in the primary shell was determined to be about four. The calculations using the cluster models can provide important information about the interaction of water molecules with the cations. Therefore, we consider the cluster model to investigate the hydrophilic properties of the cations. The optimized geometries of $X^+(H_2O)_n$ clusters ($X^+ = H_3O^+$, Li^+, and Na^+) shown in Figure 11 were close to those reported in previous calculations.[39,42] The calculated interaction energies (ΔE_{int}) are shown in Figure 12. The size of the ΔE_{int} values of the clusters including the same number of water molecules followed the trend $Li^+ \geq H_3O^+ > Na^+$. This order agrees with the observed total water content λ and the number of nonfreezing water in Table 1. The electrostatic interaction between the cation and water molecules strongly influences the amount of water uptake into the membranes and the ratio of freezing and nonfreezing water within the total water content λ. These water conditions are closely related to the transport behaviors of ions and water molecules in the membranes. Therefore, the ionic conductivity and the water self-diffusion coefficient for the membranes are strongly governed by the cation−water interactions.

5. Conclusions

The temperature dependence of the ion and water transport behaviors in perfluorosulfonated ionomer membranes, Flemion type (two different EWs), and Nafion 117 in H-, Li-, and Na-form were investigated in the fully hydrated state. The ionic conductivity for the membranes suggested that H^+ in the

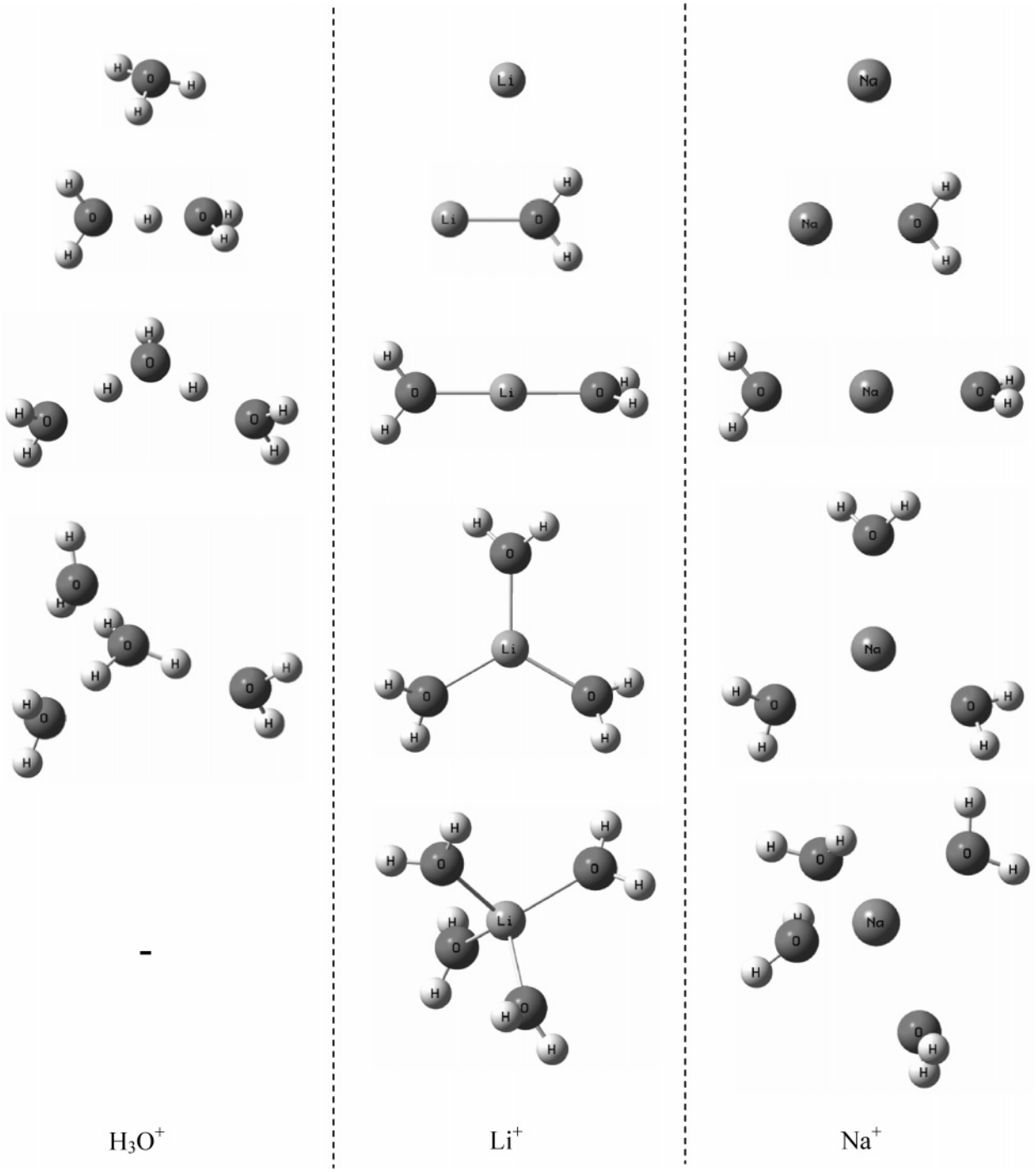

Figure 11. Optimized geometries of the $X^+(H_2O)_n$ clusters. B3LYP/6-311+G**// B3LYP/6-311+G**.

membranes transports mainly by the Grotthuss mechanism and Li^+ and Na^+ by the vehicle mechanism in the temperature range between 50 and 10 °C. In addition, the ionic conductivity for all of the membranes increased with decreasing EW value during the same temperature range. The water self-diffusion coefficient in the membranes exhibited a tendency similar to that of the ionic conductivity for the cation species and the EW value. However, no remarkable differences of D_{H2O} between H and the other cation-form membranes were observed. It indicates that water in the membranes diffuses almost in a similar way, but the H^+ transports by the Grotthuss mechanism so that H^+ conductivity is much higher than that of the other cations. Furthermore, the water self-diffusion coefficient and DSC measurements showed that a part of water in the membranes is frozen around −20 °C, but nonfreezing water remains and moves in the membranes at the lower temperature. The clear increase in the ratio of freezing water with decreasing EW value in the Li- and Na-form membranes agrees with the higher D_{H2O} value. The order of the total water content λ and the nonfreezing water exhibited the same tendency as that of the interaction (solvation) energy $|\Delta E_{int}|$ between the cation species and water molecules estimated by DFT calculation. The water conditions (the total water content λ and the ratio of freezing and nonfreezing water) in the membranes are strongly dependent on the cation species.

To achieve new advanced membranes having high performances, especially high H^+ conductivity, it is suggested that the membranes have not only a low EW value but also a high

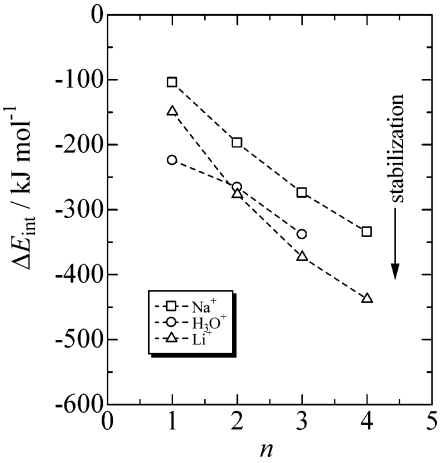

Figure 12. Interaction energies ΔE_{int} for the $X^+(H_2O)_n$ clusters. B3LYP/ 6-311+G**//B3LYP/6-311+G**.

amount of freezing water (weakly interacting water with ionic groups). Also, during the operation of PEFC, avoiding the contaminant ions such as Na^+ in the membranes is quite important.

Acknowledgment. We deeply thank Asahi Glass Co., Ltd. for supplying perfluorosulfonated ionomer membrane samples. Valuable discussions and encouragements by Dr. Seiji Tsuzuki of the same institute (AIST) are greatly acknowledged. This work was supported by New Energy and Industrial Technology Development Organization (NEDO).

References and Notes

(1) Hsu, W. Y.; Gierke, T. D. *J. Membr. Sci.* **1983**, *13*, 307.
(2) Srinivasan, S.; Manko, D. J.; Koch, H.; Enayetullah, M. A.; Appleby, J. *J. Power Sources* **1990**, *29*, 367.
(3) Heitner-Wirguin, C. *J. Membr. Sci.* **1996**, *120*, 1.
(4) *J. Membr. Sci.* **2001**, (special issue: Membranes in Fuel Cells), 185.
(5) Kreuer, K. D. In *Handbook of Fuel Cells*; Vielstich, W., Lamm, A., Gasteiger, H. A., Eds.; John Wiley & Sons Ltd.: Chichester, 2003; Vol. 3, Chapter 33, p 420.
(6) Verbrugge, M. W.; Hill, R. F. *J. Electrochem. Soc.* **1990**, *137*, 886, 893, 1131.
(7) Zawodzinski, T. A., Jr.; Neeman, M.; Sillerud, L. O.; Gottesfeld, S. *J. Phys. Chem.* **1991**, *95*, 6040.
(8) Zawodzinski, T. A., Jr.; Derouin, C.; Radzinski, S.; Sherman, R. J.; Smith, V. T.; Springer, T. E.; Gottesfeld, S. *J. Electrochem. Soc.* **1993**, *140*, 1041.
(9) Cappadonia, M.; Erning, J. W.; Stimming, U. *J. Electroanal. Chem.* **1994**, *376*, 189.
(10) Samec, Z.; Trojánek, A.; Samcová, E. *J. Electroanal. Chem.* **1995**, *389*, 1.
(11) Sone, Y.; Ekdunge, P.; Simonsson, D. *J. Electrochem. Soc.* **1996**, *143*, 1254.
(12) Samec, Z.; Trojánek, A.; Langmaier, J.; Samcavá, E. *J. Electrochem. Soc.* **1997**, *144*, 4236.
(13) Lehmani, A.; Turq, P.; Périé, M.; Périé, J.; Simonin, J.-P. *J. Electroanal. Chem.* **1997**, *428*, 81.
(14) Steck, A.; Yeager, H. L. *Anal. Chem.* **1980**, *52*, 1215.
(15) Yeager, H. L. In *Perfluorinated Ionomer Membranes*; Eisenberg, A. E., Yeager, H. L., Eds.; ACS Symposium Series 180; American Chemical Society: Washington, DC, 1982; p 25.
(16) Bontha, J. R.; Pintauro, P. N. *Chem. Eng. Sci.* **1994**, *49*, 3835.
(17) Samec, Z.; Trojánek, A.; Samcavá, E. *J. Phys. Chem.* **1994**, *98*, 6352.
(18) Pourcelly, G.; Sistat, P.; Chapotot, A.; Gavach, C.; Nikonenko, V. *J. Membr. Sci.* **1996**, *110*, 69.
(19) Tandon, R.; Pintauro, P. N. *J. Membr. Sci.* **1997**, *136*, 207.
(20) Yang, Y.; Pintauro, P. N. *AIChE J.* **2000**, *46*, 1177.
(21) Okada, T.; Kjelstrup-Ratkje, S.; Hanche-Olsen, H. *J. Membr. Sci.* **1992**, *66*, 179.
(22) Xie, G.; Okada, T. *Denki Kagaku* **1996**, *64*, 718.
(23) Okada, T.; Nakamura, N.; Yuasa, M.; Sekine, I. *J. Electrochem. Soc.* **1997**, *144*, 2744.
(24) Okada, T.; Møller-Holst, S.; Gorseth, O.; Kjelstrup-Ratkje, S. *J. Electroanal. Chem.* **1998**, *442*, 137.
(25) Okada, T.; Ayato, Y.; Yuasa, M.; Sekine, I. *J. Phys. Chem. B* **1999**, *103*, 3315.
(26) Okada, T.; Satou, H.; Okuno, M.; Yuasa, M. *J. Phys. Chem. B* **2002**, *106*, 1267.
(27) Saito, M.; Arimura, N.; Hayamizu, K.; Okada, T. *J. Phys. Chem. B* **2004**, *108*, 16064.
(28) Frisch, M. J.; Trucks, G. W.; Schlegel, H. B.; Scuseria, G. E.; Robb, M. A.; Cheeseman, J. R.; Montgomery, J. A., Jr.; Vreven, T.; Kudin, K. N.; Burant, J. C.; Millam, J. M.; Iyengar, S. S.; Tomasi, J.; Barone, V.; Mennucci, B.; Cossi, M.; Scalmani, G.; Rega, N.; Petersson, G. A.; Nakatsuji, H.; Hada, M.; Ehara, M.; Toyota, K.; Fukuda, R.; Hasegawa, J.; Ishida, M.; Nakajima, T.; Honda, Y.; Kitao, O.; Nakai, H.; Klene, M.; Li, X.; Knox, J. E.; Hratchian, H. P.; Cross, J. B.; Bakken, V.; Adamo, C.; Jaramillo, J.; Gomperts, R.; Stratmann, R. E.; Yazyev, O.; Austin, A. J.; Cammi, R.; Pomelli, C.; Ochterski, J. W.; Ayala, P. Y.; Morokuma, K.; Voth, G. A.; Salvador, P.; Dannenberg, J. J.; Zakrzewski, V. G.; Dapprich, S.; Daniels, A. D.; Strain, M. C.; Farkas, O.; Malick, D. K.; Rabuck, A. D.; Raghavachari, K.; Foresman, J. B.; Ortiz, J. V.; Cui, Q.; Baboul, A. G.; Clifford, S.; Cioslowski, J.; Stefanov, B. B.; Liu, G.; Liashenko, A.; Piskorz, P.; Komaromi, I.; Martin, R. L.; Fox, D. J.; Keith, T.; Al-Laham, M. A.; Peng, C. Y.; Nanayakkara, A.; Challacombe, M.; Gill, P. M. W.; Johnson, B.; Chen, W.; Wong, M. W.; Gonzalez, C.; Pople, J. A. *Gaussian 03*, revision B.04; Gaussian, Inc.: Pittsburgh, PA, 2003.
(29) Ransil, B. J. *J. Chem. Phys.* **1961**, *34*, 2109.
(30) Boys, S. F.; Bernardi, F. *Mol. Phys.* **1970**, *19*, 553.
(31) Thampan, T.; Malhotra, S.; Tang, H.; Datta, R. *J. Electrochem. Soc.* **2000**, *147*, 3242.
(32) Paddison, S. J.; Paul, R.; Zawodzinski, T. A., Jr. *J. Electrochem. Soc.* **2000**, *147*, 617.
(33) Silva, R. F.; Francesco, M. D.; Pozio, A. *J. Power Source* **2004**, *134*, 18.
(34) Kreuer, K. D.; Paddison, S. J.; Spohr, E.; Schuster, M. *Chem. Rev.* **2004**, *104*, 4637.
(35) Gierke, T. D.; Munn, G. E.; Wilson, F. C. *J. Polym. Sci.* **1981**, *19*, 1687.
(36) Einstein, A. *Investigations on the Theory of Brownian Movement*; Dover: New York, 1959.
(37) Hawlicka, E. *Chem. Soc. Rev.* **1995**, *34*, 13743.
(38) Balucani, U.; Vallauri, R.; Gaskell, T. *Ber. Bunsen-Ges. Phys. Chem.* **1990**, *94*, 261.
(39) Glendening, E. D.; Feller, D. *J. Phys. Chem.* **1995**, *99*, 3060.
(40) Ohtomo, N.; Arakawa, K. *Bull. Chem. Soc. Jpn.* **1979**, *52*, 2755.
(41) Eisenberg, D.; Kauzmann, W. *The Structure and Properties of Water*; Oxford University Press: London, 1969.
(42) Khan, A. *Chem. Phys. Lett.* **2000**, *319*, 440.